

研究論文

1.0Cr-1.0Mo-0.25V 터어빈 로터강의 열영향부 연화층이 크립 파단 특성에 미치는 영향

- Part II : 탄화물 형태 -

오 영근* · J.E. Indacochea**

Effect of HAZ Softening Zone on Creep Rupture Properties of 1.0Cr-1.0Mo-0.25V Turbine Rotor Steels

- Part II : Carbide Morphology -

Young Kun Oh* and J.E. Indacochea**

Key Words : Carbide Morphology (탄화물 형태), Creep Cavity (크립 기공), Carbide Extraction Replica Method (탄화물 추출 복제법)

초 록

손상된 터어빈 로터강의 보수 용접에 있어서 용접부의 크립 파단 수명과 탄화물간의 관계가 연구되었다. 탄화물은 탄화물 추출 복제법을 이용하여 확인되었으며 로터강에는 Molybdenum 주성분의 M_2C , Vanadium 주성분의 M_4C_3 및 Chromium 주성분의 $M_{23}C_6$ 와 M_7C_3 탄화물이 존재하였다. 한편 ICHAZ에서 파단된 시험편의 파단면에서는 구상의 조대한 Molybdenum 주성분의 M_6C 탄화물이 발견되었다. 조대한 Molybdenum 주성분의 M_6C 탄화물의 석출은 탄화물 주위에 고용경화 원소인 Molybdenum 농도를 떨어뜨려 기공 발생 원인을 제공하였다. CGHAZ에서 파단된 용접부의 파단면에서는 조대한 M_6C 와 $M_{23}C_6$ 가 발견되었다.

Abstract

In repaired weldment of ASTM A-470 class 8 high pressure stream turbine rotor steel, creep rupture life was studied in relation with carbide morphology. Carbides were identified using carbide extraction replica method. A retired rotor has molybdenum rich carbide (M_2C),

* 정회원, 기아자동차 (주)

** 비회원, The University of Illinois at Chicago

vanadium rich carbide (M_4C_3), and chromium rich carbides ($M_{23}C_6$ and M_7C_3). Weldments ruptured at ICHAZ showed that some of carbides have been transformed into spherical types of coarsened carbides at ruptured area. Those carbides were revealed as molybdenum rich M_6C carbide and they provided cavitation sites due to molybdenum depletion around M_6C carbide. However coarsened M_6C and $M_{23}C_6$ carbides were observed at ruptured area in case of ruptured at CGHAZ.

1. Introduction

Failure at creep condition is related to either cracking at grain boundary triple junctions or the formation of cavities (or voids) on grain boundaries which are approximately normal to the applied stress. These two types of defects are often referred to as w-type crack and r-type crack respectively¹⁾. Development of the latter type leads to premature failure of limited ductility and it is known as creep cavitation. Cavities are normally formed by grain boundary sliding causing stress concentrations at precipitates in the grain boundaries. The precipitates that provide cavity nucleation sites are mostly sulfides²⁾ and carbides^{3, 4)}. Cane and Middleton²⁾ found that all detectable sulfides appeared to nucleate cavities, however no interfacial cracking around carbides was observed. However, Myers and Pilkington⁵⁾ reported that cavitation does not occur exclusively at MnS particles and the concept of cavities being exclusively nucleated at grain boundary MnS particles is also incompatible with the cavity nucleation data obtained, i.e. there are too few MnS particles present in the grain boundaries to support the rate of cavity nucleation observed. Therefore it is clear that other grain boundary particles, including carbides, may act as cavity nucleation sites. The carbides that provide cavity sites are usually $M_{23}C_6$ ⁶⁾ and M_6C ⁷⁾. It is necessary to have carbides in sufficient numbers and size to make creep cavitation. According to Cane⁶⁾, the strain concentration factor of a boundary particle

increases with particle size and so predicted that decohesion would occur when the carbides are large.

Although considerable researches have been carried out on the carbides that provide cavitation, the detailed processes by which cavitation develops during welding remains uncertain. Some reports⁸⁻¹¹⁾ show that Cr-Mo-V steel structures fabricated by welding has a high percent of failures in the microstructurally altered and inhomogeneous HAZ. The failure takes place either at the coarse grain HAZ (CGHAZ)^{8,9)} or intercritical HAZ region (ICHAZ)^{10,11)}. It also showed that failure location changed depending on welding conditions¹²⁾. However, it is not still clear what factors control failure location, rupture life and what major mechanisms contribute creep behavior. Therefore this investigation addresses these issues which are objectives of this study: i) identify carbide morphology at creep ruptured area as a function of heat inputs and welding processes, ii) correlate carbide morphology, creep cavitation and its effect on creep rupture life and failure location.

2. Experimental Procedure

Creep rupture test specimens were used to reveal carbides and cavities. Specimens were etched using a solution of picric and tridecylbenzene sulfonate for 20 to 30 min. to exhibit creep cavities. Carbides were identified by carbide extraction replica method. Aluminum was used as the deposit material to facilitate good X-

ray analysis. Carbide analysis was carried out using a scanning transmission electron microscope equipped with energy dispersive X-ray analysis. Stable carbides around A_1 temperature were established by heat treatment in furnace. Heat treatment was conducted every 50°C from 750°C to 900°C . The holding time was 0.5h, 1h, 5h, 10h, 50h and 100h at each temperature. Precipitates were electrolytically extracted according to the ASTM procedure E963-83. This technique selectively dissolves the matrix, while leaving the precipitates unaffected and free to be filtered out of the extraction medium. X-ray powder diffraction analysis was carried out on electrolytically extracted precipitates to identify carbide type.

3. Results and Discussion

Carbide Morphology at Ruptured Area

The retired rotor steel was found to contain three types of carbides: chromium rich $M_{23}C_6$ with a small amount of M_7C_3 , molybdenum rich M_2C and vanadium rich M_4C_3 , shown in Figure 1. The stable chromium rich carbide in Cr-Mo-V steels is generally considered to be $M_{23}C_6$, but some 1Cr-Mo-V steels aged up to 103,000h at $500\text{--}600^\circ\text{C}$ have suggested that M_7C_3 may be more stable¹³. The thermodynamic data for these carbides¹⁴ suggest that the free energy of formation of $M_{23}C_6$ and M_7C_3 is similar, which implies that relatively small changes in bulk chemical compositions may significantly affect the relative stability of these chromium rich carbides. The molybdenum rich carbide M_2C is generally acicular type. M_2C appears to be the stable carbide at and below about 600°C in Cr-Mo-V steels¹⁵. The vanadium rich carbide, M_4C_3 , observed in this study is H-type. According to William et al.¹⁶, the precipitation of Mo_2C on pre-existing M_4C_3 gives rise to the H-type carbide morphology. However, R. Singh et al.¹⁷ found plate like vanadium rich carbide in 1Cr-0.3Mo-0.25V steel.

During welding, some of the carbides in the HAZ of the weld coupons of the rotor steel were transformed into stable carbide. The $M_{23}C_6$, M_7C_3 and M_4C_3 are stable carbides, but M_2C is metastable carbide. Hence, M_2C may transform into M_6C which is final stable form of molybdenum rich carbide. According to Baker and Nutting's stability diagram¹⁸, M_2C transforms into M_6C after a long period of exposure at temperature of over 700°C .

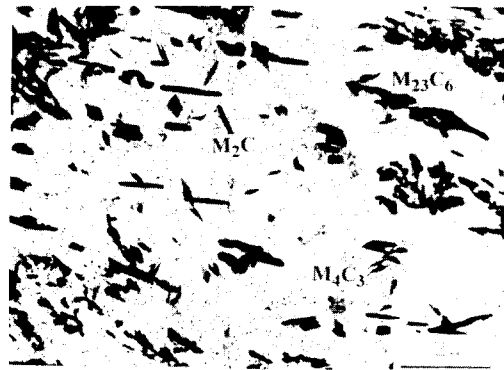
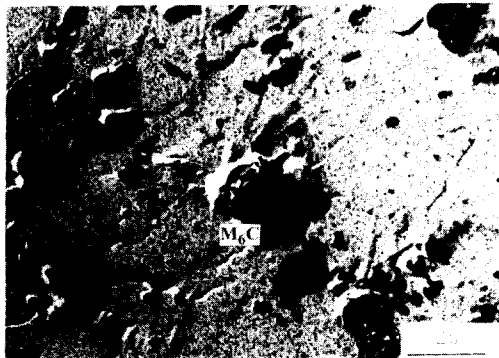


Fig. 1 Carbide morphology of as retired rotor steel

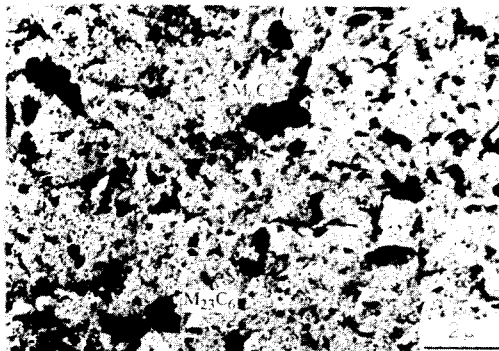
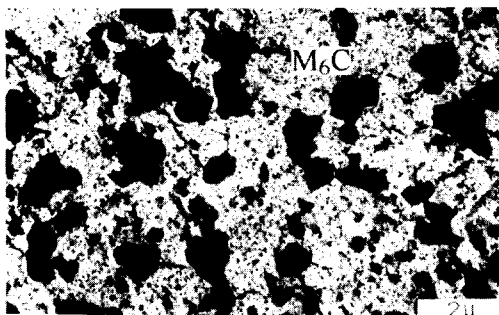
Figure 2 (a) - (c) shows carbides found at the ruptured area of creep rupture test specimens. Replicas were taken as close as possible to the ruptured area of the creep rupture specimens. Figure 2 (a) and (b) shows the carbides found in the TIG crossweld specimen that ruptured at the ICHAZ. Some carbides coarsened, while others dissolved. The coarsened carbides were identified as M_6C .

Coarsening and dissolution have been considered as separate processes, but, in practice, coarsening always precedes dissolution. This was observed in the carbides found at the ruptured area produced with different heat inputs. Most of the carbides in the 78 kJ/in heat input specimen were still coarsening and getting transformed into M_6C carbides. However the carbides in the 90 kJ/in heat input specimen were not only coarsened

but also some dissolved. This could explain why the number of coarsened carbides in the 90 kJ/in heat input specimen were less than those present in the 78 kJ/in heat input specimen.



(a)



(c)

Fig. 2 Carbide showing at ruptured area of (a) 90kJ/in, (b) 78kJ/in, and (c) 57.6kJ/in heat input TIG weld.

No vanadium rich M_4C_3 carbides could be found at the ruptured area. It means that the rupture took place at a region in the HAZ where temperature reached during welding caused the dissolution of most M_4C_3 carbides and coarsen M_6C carbides formed.

At heat input lower than 78 kJ/in, it seems that the temperature and time for carbides to coarsen at the ICHAZ are not adequate; instead, coarsened carbides formed at the CGHAZ. Figure 2(c) shows the carbide present at the CGHAZ (location of rupture). These coarse carbides were identified as M_6C and $M_{23}C_6$. The chemical composition of the M_6C and $M_{23}C_6$ is listed in Table 1.

Table 1. Chemical Compositions of M_6C and $M_{23}C_6$ Carbide, wt-%

	M_6C	$M_{23}C_6$
Chromium	5.59	35.95
Molybdenum	47.96	10.08
Vanadium	1.58	1.63
Iron	28.93	39.09
Carbon	15.94	31.25

The sequence of carbide formation on tempering up to 750°C of 2.25Cr-1Mo steel has been already established¹⁸⁾. Operation temperatures of turbine rotor are generally below 700°C, therefore this carbide stability diagram is very useful. However the temperature of failure locations, which were either ICHAZ or CGHAZ, was definitely higher than 750°C. The carbide transformation sequence over 750°C will help us to understand the mechanism of failure and so the same method was performed for retired rotor steel. Tempering temperatures were selected between 750°C and 900°C at 50°C interval and tempering times 0.5hr, 1hr, 5hr, 10hr, 50hr, and 100hr were chosen for each temperature. figure 3 shows the X-ray diffraction analysis of electrolytically extracted carbides as-retired rotor steel. Four types of

carbides, M_2C , M_4C_3 , M_7C_3 , and $M_{23}C_6$ were recognized in the as-retired rotor steel. The M_7C_3 was hardly observed by aluminum extraction replica, but it was detected by X-ray diffraction analysis. Table 2 summarizes the carbide identified in the specimens heat treated for 0.5hr and 100hr at four different tempering temperatures. No significant results in terms of carbide changes were obtained in the other tempering times. There are some significant changes in carbide types that had occurred during tempering. First, molybdenum rich M_6C carbide started to form after 100hr at 850°C. Second, vanadium rich M_4C_3 carbide completely dissolved after 0.5hr at 900°C

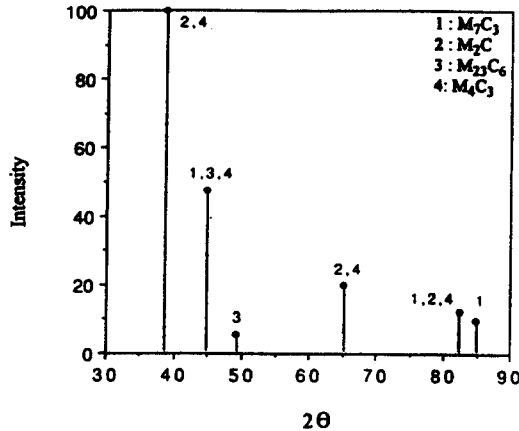


Fig. 3 X-ray diffraction analysis of electrolytically extracted carbides of as-retired rotor steel

Effect of Carbide Morphology on Creep Rupture Strength

The main factors affecting the creep strength of a low alloy ferritic/bainitic steel are primarily (i) the amount of alloying elements present in the matrix and (ii) the morphology of carbides. Substitutional alloying elements will harden the lattice by increasing the average frictional force acting on a dislocation, which in turn will increase the creep strength to some extent. The creep strength is also dependent on the presence of carbide precipitates which hinder the movement of

Table 2. Carbide morphology change with tempering temperature and time. Carbides were extracted by electrolytic method and identified by X-ray diffraction analysis

Tempering Temperature	Tempering Time	
	0.5h	100h
As-Received	M_2C , M_4C_3 , M_7C_3 , $M_{23}C_6$	
750°C	M_2C , M_4C_3 , M_7C_3 , $M_{23}C_6$	M_2C , M_4C_3 , M_7C_3 , $M_{23}C_6$
800°C	M_2C , M_4C_3 , M_7C_3 , $M_{23}C_6$	M_2C , M_4C_3 , M_7C_3 , $M_{23}C_6$
850°C	M_2C , M_4C_3 , M_7C_3 , $M_{23}C_6$	M_2C , M_4C_3 , M_7C_3 , $M_{23}C_6$, M_6C
900°C	M_2C , M_7C_3 , $M_{23}C_6$, M_6C	M_2C , M_7C_3 , $M_{23}C_6$, M_6C

the dislocations¹⁹. The highest creep strength is associated with microstructures consisting of uniformly dispersed precipitates of fine carbides, however the poorest creep properties are related with those exhibiting coarse irregularly distributed carbide precipitates.

Upon examination of the creep rupture test results, it was observed a significant difference in rupture life between the samples extracted from the as-retired rotor and the crossweldments. On examination of the carbides present at the failure surfaces, small carbides were present in the as-retired steel, while coarse and spheroidized carbides were found in the crossweldments¹². The presence of coarse carbides deteriorated the creep strength due to easy movement of the dislocations. The coarse carbides in the crossweld specimen that ruptured at the ICHAZ were identified as molybdenum rich M_6C as indicated before. Coarsening of the molybdenum rich carbides would also cause molybdenum depletion of the bainite matrix. This produces further deterioration in the creep strength, since molybdenum is a high temperature solid solution strengthener. It is obvious from this analysis that the longer rupture life experienced by the as-retired rotor is an attribute to the high creep rupture strength due to

the fine carbides present and enough molybdenum in the matrix as a solid solution strengthening. On the other hand, the ruptured area of the crossweldments showed coarse carbides combined with a depleted molybdenum in matrix.

Not only M_6C carbide but also coarse $M_{23}C_6$ carbide was found in case of specimen ruptured at CGHAZ. The coarse $M_{23}C_6$ carbide did not affect the solid solution strength in the matrix, but it resisted the movement of the dislocations. It is believed that these coarse carbides provide bainite matrix decohesion sites due to dislocation pile ups.

The creep properties of rotor steels might be related to the size and distribution of the secondary hardening precipitate, which in this material is the vanadium rich carbide M_4C_3 , high creep strength being favored by a fine uniform dispersion of this carbide. The dispersion strengthening caused by non-coherent particles is considered to be of greater significance than the strengthening of the solid solution²⁰. It was observed that M_4C_3 carbide which provides enhanced creep strength was hardly observed at the rupture area. According to William et al.¹⁶, molybdenum diffuses to M_4C_3 that slowly transforms into a molybdenum rich carbide during tempering. As much as 85 wt-% Mo could dissolve in M_4C_3 at around 600°C after extensive aging²¹. This was observed by the furnace aged specimens in this study. The molybdenum rich M_6C started to form after 100hr at 850°C with vanadium rich M_4C_3 existence. The M_4C_3 carbide completely dissolved after 0.5hr at 900°C. Complete dissolution of M_4C_3 carbide at the ruptured area seemed to contribute to deterioration in the creep strength, then rupture took place.

Creep Cavity Nucleation and Growth at Ruptured Area

Ruptured specimens were observed using SEM near the ruptured area as shown in Figure 4. The white and dark spots represent carbides and cavities respectively. Since the cavities coalesce

together during creep rupture test, inter-cavity distance is expected to influence the rupture life. If the inter-cavity distance is small or a large number of cavities exist, then cavity coalescence would occur more easily, causing a shorter rupture time. The number of cavities and inter-cavity distance were observed depending on heat inputs. The TIG crossweld with 90kJ/in had lower cavity density than 78kJ/in crossweld. Rupture time was found to increase as the cavity density decreased. The TIG crossweld with 90kJ/in and 78kJ/in had rupture time of 536.2hr and 340.0hr respectively; both specimens were tested at 593°C and 19 Ksi (132 Mpa).

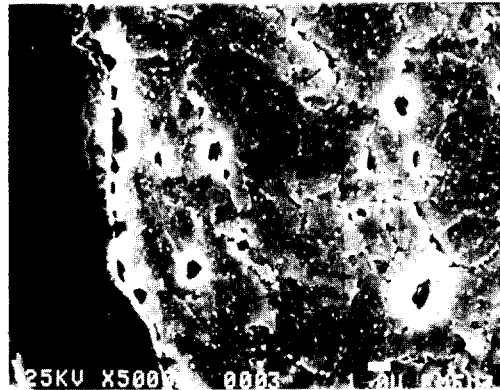


Fig. 4 Creep cavity coalesced along the ruptured area (Welding condition : 78kJ/in TIG weld)

Coarse $M_{23}C_6$ and M_6C carbides were associated with cavity nucleation sites in this study in agreement with the findings of other investigators^{6,7,22}. Coarse carbides actually initiate cavities in preference to small ones²³. Cavity nucleation are responsible for stress concentrations induced by localized deformation adjacent to carbides. The interface between grain boundary carbides and the matrix are likely to be relatively inefficient vacancy sources compared with the surrounding grain boundary. As a result, the deposition of atoms accompanying diffusional cavity growth cannot

occur uniformly and local stress concentrations will develop at the carbides. However, it appears that M_6C carbides are preferential void nucleation sites to $M_{23}C_6$ carbides, because depletion of molybdenum in the matrix due to coarsened M_6C deteriorates creep strength.

Decohesion of the ferrite-carbide interface provides the main sources of nuclei for cavity growth. The nuclei then grow considerably to develop cavities that are large enough to be connected to form a continuous crack. Most cracks propagate by the growth of microvoids ahead of a crack they finally coalesced with the main crack. Figure 5 shows the cavities around the main crack. This area is called damaged zone or bridging zone²⁴⁾. When the cavity nearest to the crack tip grows to a critical size, it is assumed to link up with the main microcrack. When microcracks connect with each other, they cause failure. The failure can usually occur by two mechanisms such as intergranular and transgranular failure. Murphy et al.²⁵⁾ reported that in Cr-Mo-V steel the fracture mode changed from transgranular dimple to intergranular wedge and then to intergranular cavitation cracking, as the applied stress is reduced. All the creep rupture test specimens in this study showed transgranular

instead of intergranular¹²⁾. The density and location of carbides also contributed to the failure mode. If there are many cavity nucleation sites in the matrix, then the failure will be transgranular, but if the matrix is relatively clean compared to the grain boundaries, then the final failure will be intergranular²⁶⁾. It was clearly showed that many coarse carbides which provide cavity nucleation sites existed in the matrix and transgranular type failure governed in this study.

4. Conclusions

Carbide morphology and creep cavity were studied in relation with creep rupture life and following conclusions were drawn:

1. The failure mechanism in all the creep rupture tests of the crossweld specimens was cavitation creep, regardless of the final fracture location.

2. The creep rupture time was also found to be affected by carbide size and population. As the weld heat input increased, the carbides coarsened to a higher degree, which caused the density of fine cavities to decrease resulting in longer creep rupture time. Coarsened carbides at the ruptured area were identified as molybdenum rich M_6C and chromium rich $M_{23}C_6$.

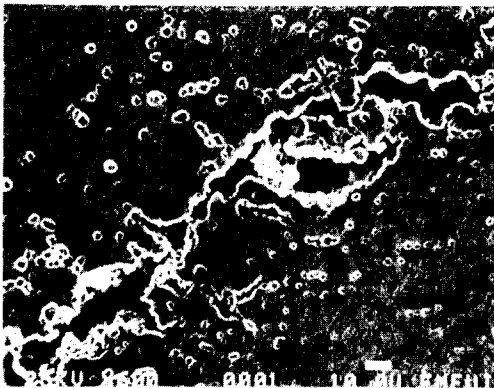


Fig. 5 Cavity formed near the main crack. This area is called damaged zone or bridging zone

References

1. F. Garofalo: *Fundamentals of Creep and Creep-Rupture*, McMillan, NY, (1965).
2. B. J. Cane and C. J. Middleton: *Met. Sci.*, Vol. 15, (1981), p. 295.
3. I. W. Chen and A. S. Argon: *Acta. Metall.*, Vol. 29, (1981), p. 1321.
4. E. P. George, P. L. Li and D. P. Pope: *Acta. Metall.*, Vol. 35, No. 10, (1987), p. 2471.
5. M. R. Myers and R. Pilkington: *Mat. Sci. & Eng.*, Vol. 95, (1987), p. 81.

6. B. J. Cane: *Met. Sci.*, Vol. 10, (1976), p. 29.
7. F. Masuyama, N. Nishimura, and Y. Takeda: *High Temp. Tech.* Vol. 8, No. 4, (1990), p. 257.
8. I. J. Chilton, A. T. Price and B. Wilshire: *Metals Tech.*, Vol. 11, (1984), p. 383.
9. K. Setoguchi, T. Daikoku, F. Masuyama, H. Haneda, and K. Muraishi : *ASME International Conference on Advances in Life Prediction Methods*, NY, USA, (1983), pp. 179-185.
10. D. J. Gooch, and S. T. Kimmins: *Proceeding of the Third International Conference on Creep and Fracture of Engineering Materials and Structures*, Swansen, U.K., Apr., (1987), pp. 689-703.
11. K. Laha, K. Bhanusankararao and S. L. Mannan: *Mat. Sci. and Eng.*, Vol. A129, (1990), p. 183.
12. Y. K. Oh: *Ph. D Dissertation at University of Illinois at Chicago*, (1993).
13. J. Maguire and D. J. Gooch: *Int. Conf. on Life Extension and Assessment*, Hague, June., (1988).
14. V. Foldyna, A. Jakobova, T. Prnka and J. Sobotka: *Proc. Conf. on the Creep Strength in Steel and High Temperature Alloys*, Sheffield, Metal Society, London, (1973), pp. 230-236.
15. R. M. Goldhoff and H. J. Beattie: *Trans. Metall. Soc. AIME*, Vol. 233, (1965), p. 1743.
16. K. R. Williams and B. Wilshire: *Mat. Sci. and Eng.*, Vol. 47, (1981), p. 151.
17. R. Singh and S. Banerjee: *Scripta Metall.*, Vol. 24, (1990), p. 1093.
18. R. G. Baker and J. Nutting: *J. Iron and Steel*, Jul., (1959), p. 257.
19. G. J. P. Buchi, J. H. R. Page, and M. P. Sidey: *JISI*, (1965), p. 291.
20. K. Laha, K. B. S. Rao and S. L. Mannan: *Proceedings of the Fifth International Conference on Creep Materials*, FL., USA, May, (1992), pp. 399-407.
21. B. A. Senior: *Mat. Sci. & Eng.*, Vol. A103, (1988), p. 263.
22. C. C. Li: *Proc. Conf. on Joining Dissimilar Metals*, Pittsburgh, PA, AWS/EPRI, (1982), pp. 107-149.
23. M. F. Ashby: *Phil. Mag.*, Vol. 14, (1966), p. 1157.
24. M. D. Thouless: *J. Am. Ceram. Soc.*, Vol. 71, No. 6, (1988), p. 408.
25. M. C. Murphy and G. D. Branch: *JISI*, Oct., (1969), p. 1347.
26. D. P. Pope: *Treatise on Materials Science and Technology*, Vol. 25, (1992), p. 125.